

# Large-scale Traffic Signal Control Using a Novel Multi-Agent Reinforcement Learning

Xiaoqiang Wang, Liangjun Ke, *Member, IEEE*, Zhimin Qiao, and Xinghua Chai

**Abstract**—Finding the optimal signal timing strategy is a difficult task for the problem of large-scale traffic signal control (TSC). Multi-Agent Reinforcement Learning (MARL) is a promising method to solve this problem. However, there is still room for improvement in extending to large-scale problems and modeling the behaviors of other agents for each individual agent. In this paper, a new MARL, called *Cooperative double Q-learning* (Co-DQL), is proposed, which has several prominent features. It uses a highly scalable independent double Q-learning method based on double estimators and the UCB policy, which can eliminate the over-estimation problem existing in traditional independent Q-learning while ensuring exploration. It uses mean field approximation to model the interaction among agents, thereby making agents learn a better cooperative strategy. In order to improve the stability and robustness of the learning process, we introduce a new reward allocation mechanism and a local state sharing method. In addition, we analyze the convergence properties of the proposed algorithm. Co-DQL is applied on TSC and tested on a multi-traffic signal simulator. According to the results obtained on several traffic scenarios, Co-DQL outperforms several state-of-the-art decentralized MARL algorithms. It can effectively shorten the average waiting time of the vehicles in the whole road system.

**Index Terms**—Traffic signal control, mean field approximation, multi-agent reinforcement learning, double estimators.

## I. INTRODUCTION

TRAFFIC congestion is becoming a great puzzling problem in urban, mainly due to the difficulty of effective utilization of limited road resources (e.g. road width). By regulating traffic flow of road network, the traffic signal control (TSC) at intersections plays an important role in utilizing the road resources and helping to reduce traffic congestion [1].

Many researchers have devoted efforts to TSC, with the aim of minimizing the average waiting time in the whole traffic system and maximizing social welfare [2]. When traffic signals are large-scale, the traditional control methods such as pre-timed [3] and actuated control systems [4] may fail to deal with the dynamic of the traffic conditions or lack the ability to foresee traffic flow. Intelligent computing methods (such as genetic algorithm [5], swarm intelligence [6], neuro-fuzzy networks [7] [8]), however, in many cases, suffer from a slow convergence rate. Reinforcement learning [9] is a promising adaptive decision-making method in many fields. It has been applied to cope with TSC [10] [11]. It can not only make

X. Wang, L. Ke and Z. Qiao are with the School of Automation, Xi'an Jiaotong University, Xi'an, Shaanxi, 710049 China (e-mail: wangxq5127@stu.xjtu.edu.cn; keljxjtu@xjtu.edu.cn; qiao.miracle@gmail.com).

X. Chai is with The 54th Research Institute of China Electronics Technology Group Corporation, Shijiazhuang, Hebei, China (e-mail:cetc54008@yeah.net).

real-time decisions according to traffic flow, but also predict future traffic flow. Especially in recent years, reinforcement learning has made tremendous progress which significantly attributes to the success of deep learning [12]. By using deep neural network to approximate the value function or action-value function (such as DQN [13], DDPG [14]), reinforcement learning can be adapted to the problems with large-scale state space or action space.

As for TSC with large-scale intersection signals, a popular idea is centralized, in which TSC is considered as a single-agent learning problem [5] [15]. However, the centralized approaches often need to collect all traffic data in the network as the global state [16], which may lead to high latency and failure rate. In addition, as the number of traffic signals increases, the joint state space and action space of the agent will also increase exponentially to a large extent, which incurs the curse of dimension. As a result, a centralized method often requires very heavy computational and communication burden.

An alternative way is multi-agent reinforcement learning (MARL) in which each signal in the traffic network is regarded as an agent. A challenge of a MARL approach is how to response to the dynamic interaction between each traffic signal and the environment, which significantly affects the adaptive decision-making of other signals [17]. Moreover, most of the current MARL methods are only studied on very limited-size traffic network problems [18] [19]. However, in urban traffic systems, it is often necessary to consider all the signals in a global coordination manner. In [20] [21], each signal is regarded as an independent agent for training. Although this kind of approaches can easily be extended to large-scale scenarios, each agent only considers its local information. Furthermore, this kind of approaches directly ignore the actions of other agents in the system and implicitly suggest that the environment is static, making it difficult for agents to learn favorable strategies with convergence guarantee. In [22], a max-plus method is proposed to deal with large-scale traffic problem, but this approach requires additional computation during execution. Multi-agent A2C [23] is developed from IA2C which is scalable and belongs to a decentralized MARL algorithm, but it may be uneasy to determine the appropriate attenuation factor to weaken the state and reward information from other agents.

In this work, we present a decentralized and scalable MARL method which is named after Cooperative double Q-learning (Co-DQL) and apply it to TSC. The new approach adopts a highly scalable independent double Q-learning method, with the aim of avoiding the problem of over estimation suffered from traditional independent Q-learning [24]. At the mean

time, it can ensure exploration by using the UCB [25] rule. In order to make agents learn a better cooperative strategy for large-scale problems, it employs mean field theory [26], which has been studied in [27]. It approximately treats the interactions within the population of agents as the interaction between a single agent and a virtual agent averaged by the other individuals in the population, which potentially transmits the action information among all agents in the environment. Furthermore, we introduce a new reward allocation mechanism and a local state sharing method to make the learning process of agents more stable and robust. To theoretically support the effectiveness of the proposed algorithm, we provide the convergence proof of the proposed algorithm under some mild conditions. Numerical experiment is performed on a multi-traffic signal simulator. Comparative results are obtained on three different traffic flow scenarios. In contrast to several reinforcement learning algorithms, the proposed method can greatly reduce the waiting time of vehicles in the whole road system.

The paper is organised into six sections. Section II describes the background on reinforcement learning. Section III presents the proposed method and analyzes the convergence properties. Section IV introduces the application of Co-DQL to TSC problem. Section V describes the setup and conditions of the experiment in detail, and makes a comparative analysis and discussion on the experimental results. Section VI summarises this paper.

## II. BACKGROUND ON REINFORCEMENT LEARNING

### A. Single-Agent RL

Q-learning is one of the most popular reinforcement learning methods and it solves sequential decision-making problems by learning estimates for the optimal value of each action. The optimal value can be expressed as  $Q^*(s, a) = \max_{\pi} Q^{\pi}(s, a)$ . However, it is not easy to learn the values of all the actions in all states when the state space or action space is larger. In this case, we can learn a parameterized action-value function  $Q(s, a; \theta)$ . When taking action  $a_t$  in state  $s_t$  and observing the immediate reward  $r_{t+1}$  and resulting state  $s_{t+1}$ , the standard Q-learning updates the parameters as follows:

$$\theta_{t+1} = \theta_t + \alpha \left( Y_t^Q - Q(s_t, a_t; \theta_t) \right) \nabla_{\theta_t} Q(s_t, a_t; \theta_t) \quad (1)$$

where  $t$  is the time step,  $\alpha$  is the learning rate and the target  $Y_t^Q$  is defined as

$$Y_t^Q \equiv r_{t+1} + \gamma \max_a Q(s_{t+1}, a; \theta_t) \quad (2)$$

where the constant  $\gamma \in [0, 1]$  is the discount factor that trades off the importance of immediate and later rewards. After updating gradually, it can converge to optimal action-value function.

Note that Q-learning approximates the value of the next state by maximizing over the estimated action values in the corresponding state, namely,  $\max_a Q_t(s_{t+1}, a; \theta_t)$  and it is an estimate of  $E\{\max_a Q_t(s_{t+1}, a; \theta_t)\}$ , which in turn is used to approximate  $\max_a E\{Q_t(s_{t+1}, a; \theta_t)\}$ . This method of approximating the maximum expected value has a positive deviation [24] [28] [29], which leads to over estimation of the optimal value and may damage the performance.

### B. Multi-Agent RL

The reinforcement learning of single agent is based on MDP theory, while for MARL, it mainly stems from Markov game [30], which generalizes the Markov Decision process (MDP) and were proposed as the standard framework for MARL [31].

We can use a tuple to formalize Markov game, namely  $(N, S, A_{1,2,\dots,N}, r_{1,2,\dots,N}, p)$ , where  $N$  being the number of agents in the game system,  $S = \{s_1, \dots, s_n\}$  is a finite set of system states,  $n$  being the number of states in the system,  $A_k$  is the action set of agent  $k \in \{1, \dots, N\}$ ;  $r_k : S \times A_1 \times \dots \times A_N \times S \rightarrow \mathbb{R}$  is the reward function of agent  $k$ , determining the immediate reward,  $p : S \times A_1 \times \dots \times A_N \rightarrow \mu(S)$  is the transition function. Each agent has its own strategy and chooses actions according to this strategy. Under the joint strategy  $\pi \triangleq (\pi_1, \dots, \pi_N)$ , at each time step, the system state is transferred by taking the joint action  $a = (a_1, \dots, a_N)$  selected according to the joint strategy and each agent receives the immediate reward as a consequence of taking the joint action. To measure the performance of a strategy, either the future discounted reward or the average reward over time can be used, depending on the policies of other agents. This results in the following definition for the expected discounted reward for agent  $k$  under a joint policy  $\pi$  and initial state  $s(0) = s \in S$ :

$$V_k^{\pi}(s) = E^{\pi} \left\{ \sum_{t=0}^{\infty} \gamma^t r_k(t+1) | s(0) = s \right\} \quad (3)$$

while the average reward for agent  $k$  under this joint policy is defined as:

$$J_k^{\pi}(s) = \lim_{T \rightarrow \infty} \frac{1}{T} E^{\pi} \left\{ \sum_{t=0}^T r_k(t+1) | s(0) = s \right\} \quad (4)$$

On the basis of Eq. (3) (the most used form), the action-value function  $Q_k^{\pi} : S \times A_1 \times \dots \times A_N \rightarrow \mathbb{R}$  of agent  $k$  under the joint strategy  $\pi$  can be written as follows according to Bellman equation:

$$Q_k^{\pi}(s, a) = r_k(s, a) + \gamma E_{s' \sim p} [V_k^{\pi}(s')] \quad (5)$$

where  $V_k^{\pi}(s) = E_{a \sim \pi} [Q_k^{\pi}(s, a)]$  and  $s'$  is the system state at the next time step. The commonly used MARL methods are generally based on Q-learning. The general multi-agent Q-learning framework is shown in Algorithm 1.

MARL enables each agent to learn the optimal strategy in order to maximize its cumulative reward. However, the value function of each agent is related to the joint strategy  $\pi$  of all agents, so it is in general impossible for all players in a game to maximize their payoff simultaneously. For MARL, an important solution concept is *Nash equilibrium*. Given these opponent strategies, the *best response* of agent  $k$  to a vector of opponent strategies is defined as the strategy  $\pi_k^*$  that achieves the maximum expected reward, which is given as follows:

$$E\{r_k | \pi_1, \dots, \pi_k, \dots, \pi_N\} \leq E\{r_k | \pi_1, \dots, \pi_k^*, \dots, \pi_N\}, \forall \pi_k \quad (6)$$

Then the *Nash equilibrium* is represented by a joint strategy  $\pi^* \triangleq (\pi_1^*, \dots, \pi_N^*)$  in which each agent acts with the *best response*  $\pi_k^*$  to others and all other agents follow the joint

**Algorithm 1:** general multi-agent Q-learning framework

---

**Input:** Initial Q value of all state-action pairs for each agent  $k$

**Output:** Convergent Q value for each agent  $k$

1 Initialize  $Q_k(s, a) = 0, \forall s, a, k$  ;

2 **while** not termination condition **do**

3   **for** all agents  $k$  **do**

4     select action  $a_k$

5     execute joint action  $a = (a_1, \dots, a_N)$ ;

6     observe new state  $s'$ , rewards  $r_k$ ;

7     **for** all agents  $k$  **do**

8        $Q_k(s, a) = (1 - \alpha)Q_k(s, a) + \alpha [r_k(s, a) + \gamma V_k(s')]$

---

policy  $\pi_{-k}^*$  of all agents except  $k$ , where the joint policy  $\pi_{-k}^* \triangleq (\pi_1^*, \dots, \pi_{k-1}^*, \pi_{k+1}^*, \dots, \pi_N^*)$ . In this case, as long as all other agents keep their policies unchanged, no agent can benefit by changing their policies. Many MARL algorithms reviewed strive to converge to *Nash equilibrium*. In addition, the Q-function will eventually converge to the *Nash Q-value*  $Q^* = (Q_1^*, \dots, Q_N^*)$  received in a *Nash equilibrium* of the game.

### III. DESCRIPTION OF THE PROPOSED METHOD

Co-DQL is developed from a new algorithm, called independent double Q-learning method, which is also firstly proposed in this paper. In the following, we first present the independent double Q-learning method, and then introduce Co-DQL, finally, we analyze its convergence properties.

#### A. Independent Double Q-learning Method

Most MARL methods are based on Q-learning. However, as described in Section II-A, traditional reinforcement learning methods cause the problem of over-estimation, which to some extent harms the performance of reinforcement learning methods. In [24], a double Q-learning algorithm is proposed, which uses double estimators instead of  $\max_a Q_t(s_{t+1}, a)$  to approximate  $\max_a E\{Q_t(s_{t+1}, a)\}$ , which is helpful to avoid the problem of over-estimation in standard Q-learning.

Inspired by independent Q-learning [21], we develop an independent double Q-learning method based on the UCB rule. For each agent  $k$ , it is associated with two different action-value functions, each of which is updated with a value from the other action-value function for the next state. More specifically, suppose that the two action-value functions are  $Q_k^a$  and  $Q_k^b$ , and one of them is randomly selected for updating each time. The updating process of the action-value function  $Q_k^a$  is as follows. Firstly, the maximal valued action  $a_k^*$  in the next state  $s'$  is selected according to the action-value function  $Q_k^a$ , namely,  $a_k^* = \arg\max_a Q_k^a(s', a)$ . Then we use the value  $Q_k^b(s', a_k^*)$  to update  $Q_k^a$

$$Q_k^a(s, a) \leftarrow Q_k^a(s, a) + \alpha (r_k + \gamma Q_k^b(s', a_k^*) - Q_k^a(s, a)) \quad (7)$$

instead of using the value  $Q_k^a(s', a_k^*) = \max_a Q_k^a(s', a)$  to update  $Q_k^a$  in independent Q-learning. The updating of  $Q_k^b$  is similar to this.

Here two multi-layer neural networks are used to fit the two Q-functions  $Q_k^a(s, a; \theta_t)$  and  $Q_k^b(s, a; \theta'_t)$ . The update mode is similar to the one of deep double Q-learning [28] and the target  $Y_{k,t} \equiv r_{k,t+1} + \gamma Q_k^b(s_{t+1}, \arg\max_a Q_k^a(s_{t+1}, a; \theta_t), \theta'_t)$ .

To balance exploration and exploitation, although  $\epsilon$ -greedy strategy is easier to implement for problems with larger state space, we prefer the UCB strategy since in the preliminary test we observe that the UCB strategy is slightly better than the  $\epsilon$ -greedy strategy. In order to make the target network update smoother, soft update is used rather than periodically copying parameters directly [13].

In this method, agent  $k$  just regards other agents as a part of the environment. Therefore, this method ignores the dynamic resulting from the actions of the other agents and the convergence is not guarantee. In order to learn a better cooperative strategies and make learning process more stable and robust, we introduce Co-DQL, which uses mean field approximation, a new reward allocation mechanism and local state sharing method.

#### B. Cooperative Double Q-learning Method

With the number of agents increasing, the dimension of joint action  $a$  increases exponentially, so when the number of agents is relatively large, it is often not feasible to directly calculate the joint action function  $Q_k(s, a)$  for each agent  $k$ . Mean field approximation is first proposed in [27] to deal with the problem. Its core idea is that the interactions within the population of agents are approximated by the interaction of an agent and the average effect of all the other agents. Specifically, a very natural approach is to decompose the joint action-value function as follows:

$$Q_k(s_k, a) = E_{l \sim d} [Q_k(s_k, a_k, a_l)] \quad (8)$$

where  $d$  is the uniform distribution of index set  $\mathcal{N}(k)$  of all other agents except agent  $k$  and the size of index sets is  $N_k = |\mathcal{N}(k)|$ .

Suppose that each agent has  $C$  discrete actions  $\{1, 2, \dots, C\}$ . Then the action of agent  $k$  can be coded using one-hot, so the mean action  $\bar{a}_k$  of all others except agent  $k$  can be expressed as:  $\bar{a}_k \triangleq [\bar{a}_{k,1}, \bar{a}_{k,2}, \dots, \bar{a}_{k,C}]$ . Accordingly, the one-hot coding action of the agent  $l$  can be expressed as:  $a_l = \bar{a}_k + \delta_{l,k}$ , where  $\bar{a}_k = E_{l \sim d} [a_l]$  and  $\delta_{l,k}$  is a small fluctuation. Under the premise of twice-differentiable, using Taylor expansion theory, the mean field approximation is expressed by the following formulate on the basis of Eq. 8:

$$Q_k(s_k, a) = E_{l \sim d} [Q_k(s_k, a_k, a_l)] \approx Q_k(s_k, a_k, \bar{a}_k) \quad (9)$$

It can be seen intuitively that the complexity of the interactions among agents is dramatically reduced. The UCB exploration strategy is used to select an action to be performed by the agent  $k$ :

$$a_k = \arg\max_{c \in \mathbf{A}_k} \left\{ Q_k(s_k, c, \bar{a}_k) + \sqrt{\frac{\ln R_{s_k, \bar{a}_k}}{R_{s_k, c, \bar{a}_k}}} \right\} \quad (10)$$

where  $R_{s_k, \bar{a}_k}$  denotes the number of times the state  $(s_k, \bar{a}_k)$  has been visited and  $R_{s_k, c, \bar{a}_k}$  denotes the number of times action  $c$  has been chosen in this state until now. If action  $c$

has been chosen rarely in some states, then the second term will dominate the first term and action  $c$  will be explored. As learning progresses, the first term dominates the second term and the UCB strategy ultimately becomes a greedy one.

For partially observable Markov traffic scenarios, each agent  $k$  can get its own reward  $r_k$  and local observation  $s_k$  at each time step. We propose to allocate each agent's reward according to the following formulate by considering all the other agents' immediate rewards, not just neighboring agents' rewards:

$$\hat{r}_k = r_k + \frac{1}{N_k} \sum_{i \in \mathcal{N}(k)} r_i \quad (11)$$

by considering all the other agents' immediate reward information equally, the learning process of agents is more stable and the information of remote agents can be well considered.

The local state sharing method is described as follows. For agent  $k$ , the average of the local state of all the other agents is taken as the additional input of agent  $k$ 's action-value function. So the state of the agent  $k$  can be expressed as

$$\hat{s}_k = \langle s_k, \frac{1}{N_k} \sum_{i \in \mathcal{N}(k)} s_i \rangle \quad (12)$$

where  $\hat{s}_k$  represents agent  $k$ 's joint state. This method can effectively share state information among agents and avoid dimension curse of joint state space. The size of the joint space does not change with the number of agents and has good scalability. These methods better guide the agents to learn the global cooperative strategy than using the spatial discount factor method [23]. Because in many cases it is beneficial to collaborate between remote agents rather than just neighbors, and information from remote agents may be more useful for cooperation among agents, such as the ring traffic scenario in Section V-B.

Based on the above introduction, *Cooperative double Q-learning* (Co-DQL) algorithm is proposed. The pseudo code of Co-DQL is given in Algorithm 2. In this algorithm, multi-layer perceptions parameterized by  $\phi$  and  $\phi_-$  are used to represent the two action-value functions of each agent. Co-DQL works as follows:

**Step 0 Initialize:** For each  $k = 1, \dots, N$ , initialize neural network parameters  $\phi_k$ ,  $\phi_{-,k}$  and initialize mean action  $\bar{a}_k$  for agent  $k$ .

**Step 1 Check the termination condition:** If a problem-specific stopping condition is met, stop and save the training neural network model.

**Step 2 Select action:** For each  $k = 1, \dots, N$ , according to the current observation  $\hat{s}_k$  of agent  $k$ , select action  $a_k$  under the UCB policy.

**Step 3 Execute action:** For each  $k = 1, \dots, N$ , agent  $k$  executes action  $a_k$  (all agents execute action synchronously), gets immediate reward  $r_k$  and next state observation  $s'_k$ .

**Step 4 Obtain samples:** For each  $k = 1, \dots, N$ , compute the mean action  $\bar{a}_k$ , reward  $\hat{r}_k$  after reallocation and next local state  $\hat{s}'_k$  after sharing.

**Step 5 Store samples in buffer:** For each  $k = 1, \dots, N$ , store the results of step 4 as a tuple sample

$\langle \hat{s}, \mathbf{a}, \hat{r}, \hat{s}', \bar{\mathbf{a}} \rangle$  in replay buffer  $\mathcal{D}_k$ ; If the number of samples stored in the  $\mathcal{D}_k$  is less than the minimum number of samples required for training, goto Step 1, otherwise the next step is executed sequentially.

**Step 6 Compute sample target values:** For each  $k = 1, \dots, N$ ,  $M$  samples are randomly extracted from  $\mathcal{D}_k$  and the target value  $Y_k^{\text{Co-DQL}}$  is calculated according to the sample data.

**Step 7 Update Neural Network Parameters:** For each  $k = 1, \dots, N$ , the gradient of the parameter  $\phi_k$  is obtained from the loss function, and  $\phi_k$  is updated according to the learning rate, then  $\phi_{-,k}$  is softly updated with update rate  $\tau$ . Goto Step 1.

For most reinforcement learning problems, the termination condition of the algorithm is generally set as the number of episodes experienced by agents to reach the maximum number of episodes. The specific value of the maximum number of episodes is usually selected according to the training situation of the algorithm in the given problem.

The action-value function  $Q_k^a(\cdot|\phi)$  (parameterized by  $\phi$ ) is trained by minimizing the loss:

$$\ell(\phi_k) = \left( Q_k^a(\hat{s}_k, a_k, \bar{a}_k; \phi) - Y_k^{\text{Co-DQL}} \right)^2 \quad (13)$$

where  $Y_k^{\text{Co-DQL}}$  is the target value of agent  $k$  and is calculated by the following formulation:

$$Y_k^{\text{Co-DQL}} = \hat{r}_k + \gamma Q_k^b(\hat{s}'_k, \text{argmax}_{a_k} Q_k^a(\hat{s}'_k, a_k, \bar{a}_k; \phi), \bar{a}'_k; \phi_-) \quad (14)$$

In Co-DQL, the mean field approximation makes every independent agent learn the awareness of collaboration with the other agents. Moreover, the reward allocation mechanism and the local state sharing method of agents improve the stability and robustness of the training process compared with the independent agent learning method.

In order to theoretically support the effectiveness of our proposed Co-DQL algorithm, we provide the convergence proof under some assumptions in the next subsection.

### C. Convergence Analysis

In previous literature, the convergence of mean field Q-learning under the set of tabular Q-functions and the convergence of when Q-function is represented by other function approximators have been proved [32] [27]. Under similar constraints, we develop the convergence proof of Co-DQL, which is a mean field reinforcement learning with double estimators.

Assuming that there are only a limited number of state-action pairs, for each agent  $k$ , we can write updating rules of two functions  $Q_k^a$  and  $Q_k^b$  of agent  $k$  according to Section III-A and Section III-B:

$$\begin{aligned} Q_k^a(s, a_k, \bar{a}_k) &\leftarrow (1-\alpha)Q_k^a(s, a_k, \bar{a}_k) + \alpha(r + \gamma Q_k^b(s', \mathbf{a}_k^*, \bar{a}_k)) \\ Q_k^b(s, a_k, \bar{a}_k) &\leftarrow (1-\alpha)Q_k^b(s, a_k, \bar{a}_k) + \alpha(r + \gamma Q_k^a(s', \mathbf{b}_k^*, \bar{a}_k)) \end{aligned} \quad (15)$$

where  $\mathbf{a}_k^* = \text{argmax}_{a_k} Q_k^a(s', a_k, \bar{a}_k)$ , and  $\mathbf{b}_k^* = \text{argmax}_{a_k} Q_k^b(s', a_k, \bar{a}_k)$ . At any update time step, either of

---

**Algorithm 2:** Co-DQL

---

**Input:** Initial parameters  $\phi$  and mean action  $\bar{a}$  for all agents

**Output:** Parameters  $\phi$  for all agents

1 Initialize  $Q_k^a(\cdot|\phi), Q_k^b(\cdot|\phi_-)$  and  $\bar{a}_k$  for all  $k \in \{1, \dots, N\}$

2 **while** not termination condition **do**

3 For each agent  $k$ , select action  $a_k$  using the UCB exploration strategy from Eq. 10

4 Take the joint action  $a = (a_1, \dots, a_N)$  and observe the reward  $r = (r_1, \dots, r_N)$  and the next observations  $s' = (s'_1, \dots, s'_N)$

5 Compute  $\bar{a}, \hat{r}, \hat{s}$  and  $\hat{s}'$

6 Store  $\langle \hat{s}, a, \hat{r}, \hat{s}', \bar{a} \rangle$  in replay buffer  $\mathcal{D}$

7 **for**  $k = 1$  to  $N$  **do**

8 Sample  $M$  experiences  $\langle \hat{s}, a, \hat{r}, \hat{s}', \bar{a} \rangle$  from  $\mathcal{D}$

9 Compute target value  $Y_k^{\text{Co-DQL}}$  by Eq. 14

10 Update the  $Q$  network by minimizing the loss

$$\mathcal{L}(\phi_k) = \frac{1}{M} \sum \left( Q_k^a(\hat{s}_k, a_k, \bar{a}_k; \phi) - Y_k^{\text{Co-DQL}} \right)^2$$

11 Update the parameters of the target network for each agent  $k$  with updating rate  $\tau$

$$\phi_k^- \leftarrow \tau \phi_k + (1 - \tau) \phi_k$$


---

the two of Eq. 15 is updated. Our goal is to prove that both  $\mathbf{Q}^a = (Q_1^a, \dots, Q_N^a)$  and  $\mathbf{Q}^b = (Q_1^b, \dots, Q_N^b)$  converge to Nash Q-values. Our proof follows the convergence proof framework of single agent Double Q-learning [24], and we use the following assumptions and lemma.

**Assumption 1.** Each action-value pair is visited infinitely often, and the reward is bounded by some constant  $K$ .

**Assumption 2.** Agent's policy is Greedy in the Limit with Infinite Exploration (GLIE). In the case with the Boltzmann policy, the policy becomes greedy w.r.t. the  $Q$ -function in the limit as the temperature decays asymptotically to zero.

**Assumption 3.** For each stage game  $[Q_t^1(s), \dots, Q_t^N(s)]$  at time  $t$  and in state  $s$  in training, for all  $t, s, j \in \{1, \dots, N\}$ , the Nash equilibrium  $\pi_* = [\pi_*^1, \dots, \pi_*^N]$  is recognized either as 1) the global optimum or 2) a saddle point expressed as:

- 1)  $\mathbb{E}_{\pi_*} [Q_t^j(s)] \geq \mathbb{E}_{\pi} [Q_t^j(s)], \forall \pi \in \Omega(\prod_k \mathcal{A}^k);$
- 2)  $\mathbb{E}_{\pi_*} [Q_t^j(s)] \geq \mathbb{E}_{\pi^j} \mathbb{E}_{\pi_*^{-j}} [Q_t^j(s)], \forall \pi^j \in \Omega(\mathcal{A}^j) \text{ and}$
- 3)  $\mathbb{E}_{\pi_*} [Q_t^j(s)] \leq \mathbb{E}_{\pi_*^{-j}} \mathbb{E}_{\pi^j} [Q_t^j(s)], \forall \pi^{-j} \in \Omega(\prod_{k \neq j} \mathcal{A}^k).$

**Lemma 1.** The random process  $\{\Delta_t\}$  defined in  $\mathbb{R}$  as

$$\Delta_{t+1}(x) = (1 - \alpha_t(x)) \Delta_t(x) + \alpha_t(x) F_t(x)$$

converges to zero with probability 1 (w.p.1) when

- 1)  $0 \leq \alpha_t(x) \leq 1, \sum_t \alpha_t(x) = \infty, \sum_t \alpha_t^2(x) < \infty;$
- 2)  $x \in \mathcal{X}$ , the set of possible states, and  $|\mathcal{X}| < \infty$ ;
- 3)  $\|\mathbb{E}[F_t(x)|\mathfrak{I}_t]\|_W \leq \gamma \|\Delta_t\|_W + c_t$ , where  $\gamma \in [0, 1)$  and  $c_t$  converges to zero w.p.1;
- 4)  $\text{var}[F_t(x)|\mathfrak{I}_t] \leq K(1 + \|\Delta_t\|_W^2)$  with constant  $K > 0$ .

Here  $\mathfrak{I}_t$  denotes the filtration of an increasing sequence of  $\sigma$ -fields including the history of processes;  $\alpha_t, \Delta_t, F_t \in \mathfrak{I}_t$  and  $\|\cdot\|_W$  is a weighted maximum norm [30].

*Proof.* Similar to the proof of Theorem 1 in [33] and Corollary 5 in [34].  $\square$

Our theorem and proof sketches are as follows:

**Theorem 1.** In a finite-state stochastic game, if Assumption 1, 2 & 3, and Lemma 1's first and second conditions are met, then both  $\mathbf{Q}^a$  and  $\mathbf{Q}^b$  as updated by the rule of Algorithm 2 in Eq. 15 will converge to the Nash  $Q$ -value  $\mathbf{Q}^* = (Q_1^*, \dots, Q_N^*)$  with probability one.

*Proof.* We need to show that the third and fourth conditions of Lemma 1 hold so that we can apply it to prove Theorem 1. Obviously, the updates of functions  $\mathbf{Q}^a$  and  $\mathbf{Q}^b$  are symmetrical, so as long as one of them is proved to converge, the other must converge. By subtracting two sides of Eq. 15 by  $\mathbf{Q}^*$ , and then the following formula can be obtained by comparing with the equation in Lemma 1:

$$\begin{aligned} \Delta_t(s, a) &= \mathbf{Q}_t^a(s, a) - \mathbf{Q}_*^a(s, a) \\ F_t(s_t, a_t) &= r_t + \gamma \mathbf{Q}_t^b(s_{t+1}, a^*) - \mathbf{Q}_*^b(s_t, a_t) \end{aligned} \quad (16)$$

where  $a^* = \text{argmax}_a \mathbf{Q}^a(s_{t+1}, a_t, \bar{a}_t)$ . Let  $\mathfrak{I}_t = \{\mathbf{Q}_0^a, \mathbf{Q}_0^b, s_0, a_0, \alpha_0, r_1, s_1, \dots, s_t, a_t\}$  denote the  $\sigma$ -fields generated by all random variables in the history of the stochastic game up to time  $t$ . Note that  $\mathbf{Q}_t^a$  and  $\mathbf{Q}_t^b$  are two random variables derived from the historical trajectory up to time  $t$ . Given the fact that all  $\mathbf{Q}_\tau^a$  and  $\mathbf{Q}_\tau^b$  with  $\tau < t$  are  $\mathfrak{I}_t$ -measurable, both  $\Delta_t$  and  $F_t$  are therefore also  $\mathfrak{I}_t$ -measurable.

Since the reward is bounded by some constant  $K$  in Assumption 1, then  $\text{Var}[r_t] < \infty$ , the fourth condition in the lemma holds.

Next, we show that the third condition of the lemma holds. We can rewrite Eq. 16 as follows:

$$F_t(s_t, a_t) = F_t^Q(s_t, a_t) + \gamma (\mathbf{Q}_t^b(s_{t+1}, a^*) - \mathbf{Q}_t^a(s_{t+1}, a^*)) \quad (17)$$

where  $F_t^Q = r_t + \gamma \mathbf{Q}_t^a(s_{t+1}, a^*) - \mathbf{Q}_t^a(s_t, a_t)$  is the value of  $F_t$  if normal MF-Q would be under consideration. In [17],  $\|\mathbb{E}[F_t^Q|\mathfrak{I}_t]\|_W \leq \gamma \|\Delta_t\|_W$  has been proved, so in order to meet the third condition, we identify  $c_t = \gamma (\mathbf{Q}_t^b(s_{t+1}, a^*) - \mathbf{Q}_t^a(s_{t+1}, a^*))$  and it is sufficient to show that  $\Delta_t^{\text{ba}} = \mathbf{Q}_t^b - \mathbf{Q}_t^a$  converges to zero. The update of  $\Delta_t^{\text{ba}}$  depends on whether  $\mathbf{Q}^b$  or  $\mathbf{Q}^a$  is updated, so

$$\begin{aligned} \Delta_{t+1}^{\text{ba}}(s_t, a_t) &= \Delta_t^{\text{ba}}(s_t, a_t) + \alpha_t F_t^b(s_t, a_t), \text{ or} \\ \Delta_{t+1}^{\text{ba}}(s_t, a_t) &= \Delta_t^{\text{ba}}(s_t, a_t) - \alpha_t F_t^a(s_t, a_t) \end{aligned} \quad (18)$$

where  $F_t^a(s_t, a_t) = r_t + \gamma \mathbf{Q}_t^b(s_{t+1}, a^*) - \mathbf{Q}_t^a(s_t, a_t)$  and  $F_t^b(s_t, a_t) = r_t + \gamma \mathbf{Q}_t^a(s_{t+1}, b^*) - \mathbf{Q}_t^b(s_t, a_t)$ . We define

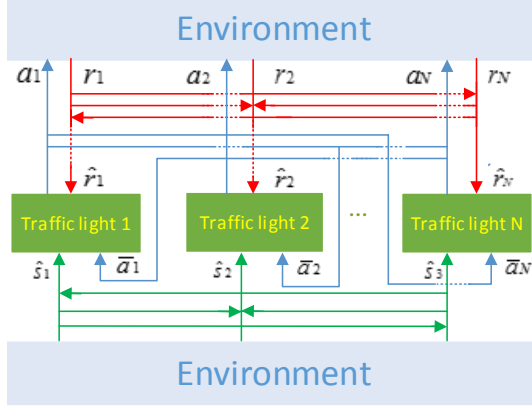


Fig. 1. The architecture diagram of Co-DQL for TSC. For each  $k = 1, \dots, N$ ,  $\hat{s}_k$  denotes the local state information after sharing,  $\bar{a}_k$  represents the mean action information,  $a_k$  means the action will be executed,  $r_k, \hat{r}_k$  represent the immediate reward before and after reallocation, respectively. The red arrow represents the transfer of reward information, the blue arrow represents the transfer of action information, and the green arrow represents the transfer of state information. The dotted line indicates disjoint.

$\xi_t^{ba} = \frac{1}{2}\alpha_t$ , then

$$\begin{aligned} \mathbb{E}[\Delta_{t+1}^{ba}(s_t, a_t) | \mathfrak{S}_t] &= \Delta_t^{ba}(s_t, a_t) + \mathbb{E}[\alpha_t \mathbf{F}_t^b(s_t, a_t) \\ &\quad - \alpha_t \mathbf{F}_t^a(s_t, a_t) | \mathfrak{S}_t] \\ &= \Delta_t^{ba}(s_t, a_t) + \mathbb{E}[\alpha_t \gamma(Q_t^a(s_{t+1}, b^*) \\ &\quad - Q_t^-(s_{t+1}, a^*)) - \alpha_t(Q_t^b(s_t, a_t) \\ &\quad - Q_t^a(s_t, a_t)) | \mathfrak{S}_t] \\ &= (1 - \xi_t^{ba}(s_t, a_t)) \Delta_t^{ba}(s_t, a_t) \\ &\quad + \xi_t^{ba}(s_t, a_t) \mathbb{E}[\mathbf{F}_t^{ba}(s_t, a_t) | \mathfrak{S}_t] \end{aligned}$$

where  $\mathbb{E}[\mathbf{F}_t^{ba}(s_t, a_t) | \mathfrak{S}_t] = \gamma \mathbb{E}[Q_t^a(s_{t+1}, a^*) - Q_t^b(s_{t+1}, a^*) | \mathfrak{S}_t]$ . At each time step, one of the following two cases must hold.

Case 1:  $\mathbb{E}[Q_t^a(s_{t+1}, b^*) | \mathfrak{S}_t] \geq \mathbb{E}[Q_t^b(s_{t+1}, a^*) | \mathfrak{S}_t]$ . We have  $Q_t^a(s_{t+1}, a^*) = \max Q_t^a(s_{t+1}, a) \geq Q_t^a(s_{t+1}, b^*)$ , therefore

$$\begin{aligned} \mathbb{E}[\mathbf{F}_t^{ba}(s_t, a_t) | \mathfrak{S}_t] &= \gamma \mathbb{E}[Q_t^a(s_{t+1}, b^*) - Q_t^b(s_{t+1}, a^*) | \mathfrak{S}_t] \\ &\leq \gamma \mathbb{E}[Q_t^a(s_{t+1}, a^*) - Q_t^b(s_{t+1}, a^*) | \mathfrak{S}_t] \\ &\leq \|\Delta_t^{ba}\| \end{aligned}$$

Case 2:  $\mathbb{E}[Q_t^a(s_{t+1}, b^*) | \mathfrak{S}_t] < \mathbb{E}[Q_t^b(s_{t+1}, a^*) | \mathfrak{S}_t]$ . We have  $\mathbb{E}[Q_t^b(s_{t+1}, b^*) | \mathfrak{S}_t] \geq \mathbb{E}[Q_t^b(s_{t+1}, a^*) | \mathfrak{S}_t]$ . Then

$$\begin{aligned} \mathbb{E}[\mathbf{F}_t^{ba}(s_t, a_t) | \mathfrak{S}_t] &= \gamma \mathbb{E}[Q_t^b(s_{t+1}, b^*) - Q_t^a(s_{t+1}, b^*) | \mathfrak{S}_t] \\ &\leq \gamma \mathbb{E}[Q_t^b(s_{t+1}, b^*) - Q_t^a(s_{t+1}, b^*) | \mathfrak{S}_t] \\ &\leq \|\Delta_t^{ba}\| \end{aligned}$$

Hence, no matter which of the above cases is hold, we can obtain the satisfactory result, that is,  $|\mathbb{E}[\mathbf{F}_t^{ba}(s_t, a_t) | \mathfrak{S}_t]| \leq \|\Delta_t^{ba}\|$ . Then, we can apply Lemma 1 and get the convergence of  $\Delta_t^{ba}$  to 0, the third condition is thus hold. Finally, with all conditions are satisfied, Theorem 1 is proved.  $\square$

#### IV. APPLICATION OF CO-DQL TO TSC

This section first uses MDP notations to represent the key elements of the problem of TSC, so that Co-DQL can be used in TSC. To facilitate the training and evaluation of the model

applied to the problem of TSC, we also introduce the simulator of signal control.

##### A. Description of TSC Based on MDP Notations

Although we model the entire traffic network in a decentralized way as a multi-agent structure, the global state of the whole traffic system is still Markov, namely, the next state only depends on the current state:

$$s_{t+1} = f(s_t, a_t) \quad (19)$$

where  $s_t$  and  $s_{t+1}$  denotes the state of traffic system at time step  $t$  and  $t + 1$ ,  $a_t$  denotes the joint action of the traffic system at time step  $t$ . Therefore, it can be modeled using the framework of MARL described in Section II-B. Fig. 1 shows the structure of applying Co-DQL to TSC. Numbered from 1 to  $N$ , each traffic light represents an agent. The input information of each agent includes the shared local state information and the mean action information calculated from actions of the other agents in the previous time step. The action output by the agent interacts with the environment, then the agent gets the immediate reward after reallocation. The red arrow represents the transfer of reward information, the blue arrow represents the transfer of action information, and the green arrow represents the transfer of state information. The dotted line indicates disjoint.

The action of signal agent  $k$  at time step  $t$  can be written as  $a_{k,t}$ , and its local observation or state is  $s_{k,t}$ . We set the signal agent's actions at each intersection has only two possible cases  $\{0, 1\}$ : Green traffic lights for incoming traffic in the north and south directions and red traffic lights in the east and west directions at the same time, or contrary to that, so the action space is  $\{0, 1\}^{m^2}$ . The local state, which is the observation vector  $s_{k,t}$ , is the waiting queue density (or queue length) on all the one-way lanes (or edges) from its neighbors to the intersection  $k$ :  $s_{k,t} = [q_{kn}, q_{ks}, q_{kw}, q_{ke}]$ , where  $q_{kn}, q_{ks}, q_{kw}$  and  $q_{ke}$  represent the waiting queue density in four directions related to intersection  $k$  respectively, and they are the lanes of vehicles driving in the direction of intersection  $k$ . The value space of each of them can be expressed as  $\{0, 1, 2, \dots, \max_q\}$ , where  $\max_q$  is the maximum capacity of vehicles on an lane between every two intersections. For the peripheral signal agent of the system, if there is no road connected to it in a certain direction, the number of vehicles in that direction is always zero. For simplicity, it is assumed that a normally traveling vehicle has the same speed and can start or stop immediately.

For any intersection signal agent  $k$ , the reward at time step  $t$  can be calculated by the number of vehicles waiting on all lanes towards the intersection, that is,

$$r_{k,t} = \sum_{j \in \{n, s, w, e\}} |q_{kj}(t)| \quad (20)$$

where  $q_{kj}(t)$  is the number of vehicles that have zero speed on lane  $kj$  leading to intersection  $k$ . To avoid changing traffic signal too frequently, the action can be taken every  $\Delta t$  time steps, that is, a Markov state transition occurs only once every  $\Delta t$  time steps. Then from the  $T$ -th to  $T + 1$ -th state transition,

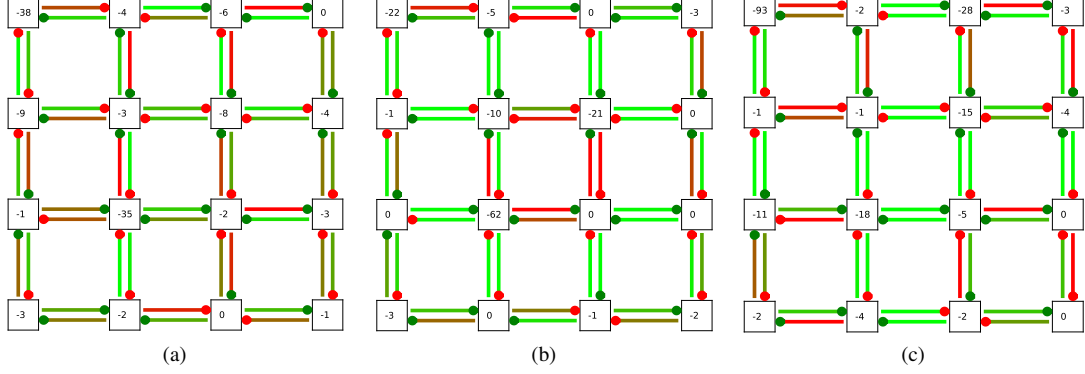


Fig. 2. Illustration of the grid traffic signal system simulator. (a) global random traffic flow, (b) double-ring traffic flow, and (c) four-ring traffic flow. Each rectangle represents an intersection and each two adjacent intersections are connected by two one-way lanes. The color of each lane implies the degree of congestion on the road at the moment and the number in the rectangle represents the immediate reward for the current time step at the intersection.

TABLE I  
PARAMETER SETTINGS FOR SIMULATOR

Parameter Type	Value [unit of measure]
Normal driving time between two nodes	5 [t]
Initial vehicles in simulator	100 [veh]
New vehicles added	5;4;3 [veh/t]
Shortest route length	2 [n]
Longest route length	20 [n]
Signal agent action time interval	4 [t]
Initial random seed number	10

$t$  means discrete time step,  $veh$  is the abbreviation of vehicle,  $n$  denotes node, i.e. intersection. 5;4;3 [veh/t] means that the number of new vehicles added per time step is optional and can be set to 5,4 or 3 as needed.

the intersection signal agent obtains the sum of the rewards in  $\Delta t$  time steps, that is,

$$R_T = \sum_{t=(T-1)\Delta t}^{T\Delta t-1} r_t(s_t, a_t) \quad (21)$$

Our goal is to minimize the total waiting time of vehicles in the transportation system:

$$\min_{\pi} J = \mathbb{E} \left[ \sum_{T=1}^{T_{max}} \gamma^{T-1} \left( \frac{1}{\Delta t} \sum_{t=(T-1)\Delta t}^{T\Delta t-1} r_t(s_t, a_t) \right) \right] \quad (22)$$

where  $T_{max}$  denotes the total number of state transitions, and the joint action  $a$  changes every  $\Delta t$  time steps.

### B. Description of the Simulation Platform

The simulation platform used in this experiment is a grid TSC system based on OpenAI-gym [35]. There are three different scenarios in the experiment: global random traffic flow, double-ring traffic flow and four-ring traffic flow which correspond to the three subfigures of Fig. 2 respectively.

Any rectangle  $k$  represents an intersection, i.e., a signal agent. The number in the rectangle represents the immediate reward for the current time step at the intersection. Every two adjacent intersections are connected by two one-way lanes.

The color of each lane in the picture ranges from green to red, which vaguely indicates the number of vehicles waiting (at zero speed) on the lane. Therefore, the color of the lane to some extent indicates the degree of congestion. Green means unimpeded and red indicates serious congestion. During the operation of the simulator, a certain number of vehicles will be generated at each time step and scattered randomly in the road network. The initial location of a vehicle in the road network is the starting point of the vehicle. At the same time, every newly generated vehicle will have a randomly generated route according to a certain rule, and the vehicle will follow the route under the restriction of traffic signals and finally it will be removed from the road network when it reaches the destination.

Among these three scenarios, the one difference is that the rules of generating a driving route of a vehicle, which results in different level of congestion at different intersections. This can simulate the real information of the traffic flow between the main and secondary roads in the city. In the actual traffic network, serious congestion does often occur only in certain specific sections. The other difference is that the number of new vehicles added per time step is various, which can be used to simulate different levels of traffic congestion.

The primary parameters of the simulator are listed in Table I. The normal driving time between two intersections, that is, the distance between two intersections, indicates that normal driving vehicles need 5 time steps from one intersection to an adjacent intersection. The initial number (note that it is not the number after resetting the simulator when training model) of vehicles in simulator is used to obtain random seeds. The shortest route length is 2, which means that the shortest distance that a vehicle generated in the simulator can travel is two intersections. The longest route length is 20, which means that the longest distance that a vehicle generated in the simulator can travel is twenty intersections. The action time interval of signal agent is 4, which means that a signal agent must keep at least 4 time steps before it can change one action.

## V. NUMERICAL EXPERIMENTS AND DISCUSSIONS

### A. Implementation Details of Algorithms

In order to analyze the performance of the proposed algorithm, we compared it with several popular reinforcement learning methods in the same traffic scenarios. Details of the implementation of Co-DQL and the other methods are described as follows:

**Co-DQL:** The procedure described in Section III-B is implemented. Multilayer fully connected neural network is used to approximate the Q-function of each agent. We use the ReLU-activation between hidden layers, and transform the final output of Q-network with it. All agents share the same Q-network, the shared Q-network takes an agent embedding as input and computes Q-value for each candidate action. We also feed in the action approximation  $\bar{a}_k$  and sharing joint state  $\hat{s}_k$ . We use the Adam optimizer with a learning rate of 0.0001. The discounted factor  $\gamma$  is set to be 0.95 and the mini-batch size is 1024. The size of replay buffer is  $5 \times 10^5$  and  $\tau = 0.01$  for updating the target networks. The network parameters will be updated once an episode samples are added to the replay buffer.

**Multi-Agent A2C (MA2C):** The start-of-the-art MARL (decentralized) algorithms for large-scale TSC. The hyper-parameters of the algorithm in this experiment are basically consistent with the original one [23].

**Independent Q-learning (IQL):** It has almost the same hyper-parameters settings as Co-DQL. And the network architecture is identical Co-DQL, except a mean action and sharing joint state are not fed as an addition input to the Q-network.

**Independent double Q-learning (IDQL):** The parameter setting of this method is almost the same as that of independent Q-learning. The main difference is that the double estimators are used when calculating the target value.

**Deep deterministic policy gradient (DDPG):** This is an off-policy algorithm too. It consists of two parts: actor and critic. Each agent is trained with DDPG algorithm and we share the critic among all agents in each experiment and all of the actors are kept separate. It uses the Adam optimizer with a learning rate of 0.001 and 0.0001 for critics and actors respectively. The settings of other parameters are the same as those of Co-DQL.

It is noteworthy that all the hyper-parameter settings of all algorithms may affect the performance of the algorithm to a certain extent.

### B. Experiments in Different Scenarios

By training and evaluating the proposed method in different traffic scenarios, we can further demonstrate that the proposed method has good generality. Next, we will analyze the performance of the algorithms in three scenarios.

1) *global random traffic flow*: As shown in the Fig. 3 (a), under the condition that signal agents adopt a random strategy, the mean reward reaches stable after about 2000 time steps, which means that the traffic flow of the simulator reaches a stable state too. In order to ensure the diversity of training samples and avoid over-fitting some traffic flow states as far as possible, we record 10 discrete simulator states (i.e. vehicle position, driving status, signal status) after 2000 time steps

TABLE II  
MODEL PERFORMANCE IN GLOBAL RANDOM TRAFFIC FLOW SCENE

Method	Average Delay Time [t]	Mean Episode Reward
IQL	148.500( $\pm 8.963$ )	-11.602( $\pm 0.700$ )
IDQL	131.854( $\pm 7.534$ )	-10.301( $\pm 0.589$ )
DDPG	111.057( $\pm 0.606$ )	-8.676( $\pm 0.047$ )
MA2C	71.553( $\pm 0.5812$ )	-5.590( $\pm 0.045$ )
Co-DQL	36.981( $\pm 0.509$ )	-2.889( $\pm 0.040$ )

*t* means discrete time step.

TABLE III  
MODEL PERFORMANCE IN DOUBLE-RING TRAFFIC FLOW SCENE

Method	Average Delay Time [t]	Mean Episode Reward
IQL	89.838( $\pm 5.645$ )	-5.615( $\pm 0.353$ )
IDQL	83.921( $\pm 2.273$ )	-5.245( $\pm 0.142$ )
DDPG	86.581( $\pm 1.182$ )	-5.411( $\pm 0.074$ )
MA2C	58.857( $\pm 0.779$ )	-3.679( $\pm 0.049$ )
Co-DQL	26.046( $\pm 0.751$ )	-1.628( $\pm 0.047$ )

*t* means discrete time step.

as random seeds and it will be used to train and evaluate these methods. In the global random traffic flow, we set the number of new vehicles added at each time step to 5, which corresponds to a high level of traffic congestion.

**Result Analysis.** We run 2500 episodes for training all five models, and regularly save the trained models. The mean reward curve of signal agents is shown in Fig. 4. It can be seen from the figure that IQL suffers the lowest training performance. Although IDQL is just slightly better than IQL, the results tend to indicate that overestimation of action-value function will damage the performance of signal control and that using double estimators can improve the performance to a certain extent. Interestingly, the performance of DDPG is better than that of IDQL. We speculate that all agents sharing critic network can implicitly transfer information, which is beneficial to the cooperation among agents. Although MA2C and Co-DQL both have more robust learning ability, Co-DQL greatly outperforms all the other methods. Co-DQL uses mean field approximation to directly model the strategies of other agents, thus it can learn a good cooperative strategies and minimize the total vehicle delay time of the whole transportation system.

For each algorithm, the best model obtained in the training process is used to test in this scenario. We evaluate all of them over 100 episodes. Table II shows the results of evaluation. Average delay time is calculated from the total delay time of vehicles in the whole transportation system during a complete episode. The standard deviation is given in parentheses after the mean value. Co-DQL greatly reduces the average delay time compared with the other methods. The results are basically consistent with the trained model performance, which shows the validity of our trained model.

2) *double-ring traffic flow* : Fig. 3 (b) shows the mean reward curve of agents using random strategies in double-ring traffic flow scene. Similarly, 10 simulator states are selected as seeds. In this scenario, we set the number of new vehicles

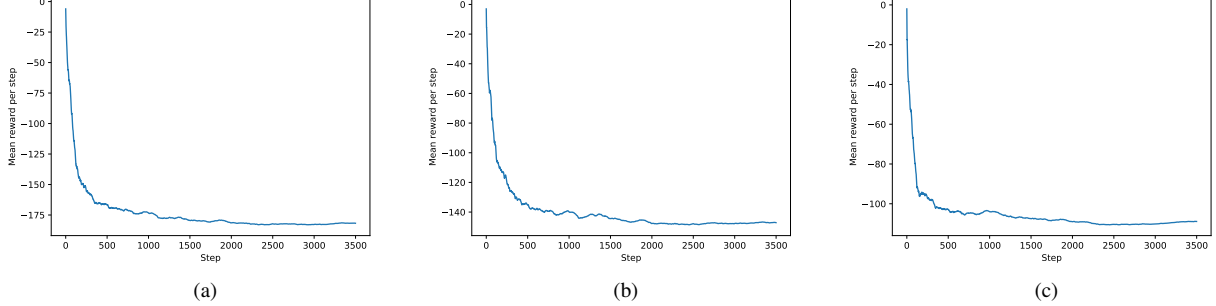


Fig. 3. Illustration of mean reward change curve of signal agents using random strategy in various traffic flows scenarios. (a) mean reward change curve of signal agent in global random traffic flow scene, (b) mean reward change curve of signal agent in double-ring traffic flow scene, and (c) mean reward change curve of signal agent in four-ring traffic flow scene. At the beginning, there are fewer vehicles running in the simulator. With the addition of a certain number of vehicles to the simulator at each time step, the level of congestion is getting worse and worse, and the mean rewards for signal agents are getting smaller and smaller. As the vehicle arriving at the destination will be removed from the simulator, the traffic flow in the simulator will reach a stable range. We intercept a certain number of simulator states after traffic flow stabilization as the initial state distribution of the simulator when training and evaluating our methods.

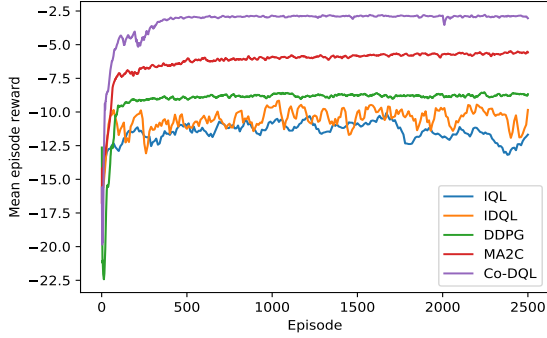


Fig. 4. Reward curve of signal agent during training in the global random traffic flow scene.

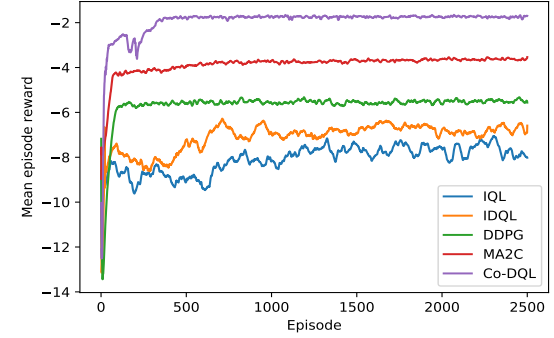


Fig. 6. Reward curve of signal agent during training in the four-ring traffic flow scene.

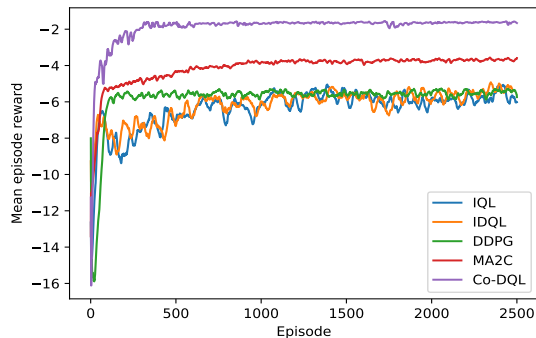


Fig. 5. Reward curve of signal agent during training in the double-ring traffic flow scene.

added to the network at each time step to 4, which corresponds to a medium level of traffic congestion. The other parameters of the simulator and all the algorithms are the same as those in Section V-B1.

**Result Analysis.** Similarly, we train all the models in this scenario and save the model with the best training performance. The mean reward curve is shown in Fig. 5. As

TABLE IV  
MODEL PERFORMANCE IN FOUR-RING TRAFFIC FLOW SCENE

Method	Average Delay Time [t]	Mean Episode Reward
IQL	168.526( $\pm 2.673$ )	-7.900( $\pm 0.125$ )
IDQL	143.986( $\pm 3.761$ )	-6.749( $\pm 0.176$ )
DDPG	116.823( $\pm 1.610$ )	-5.476( $\pm 0.075$ )
MA2C	77.633( $\pm 0.660$ )	-3.639( $\pm 0.031$ )
Co-DQL	37.174( $\pm 0.937$ )	-1.743( $\pm 0.044$ )

*t* means discrete time step.

expected, the training performance of Co-DQL method still outperforms all the other methods. In addition, mainly due to the information transfer among agents, MA2C can obtain better training results in contrast to the independent agent methods, that is, IQL and IDQL. However, although the convergence rates of DDPG, IQL and IDQL are different, the final training results are basically similar. This may be because the problem of double-ring traffic flow is relatively simple, so these three methods can achieve relatively consistent results and the overestimation of IQL does not significantly affect the performance. In this scenario, the evaluation results are shown in Table III. Co-DQL can obtain shorter average delay time and smaller standard deviations than other methods.

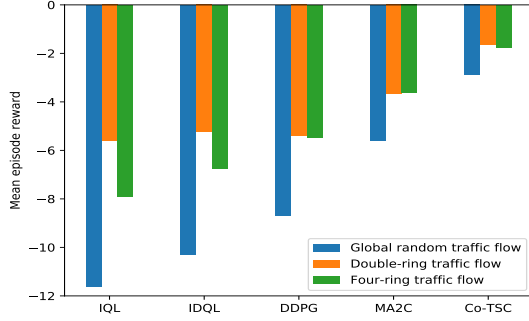


Fig. 7. Mean Episode Reward Comparison for Testing the Corresponding Model in Different Traffic Flow Scenarios.

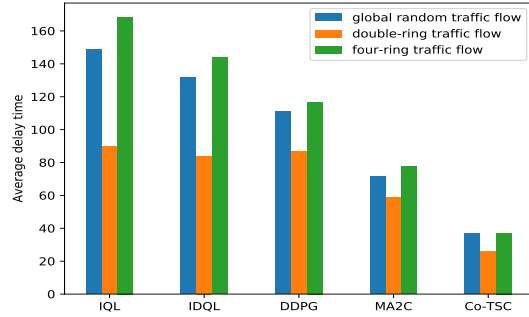


Fig. 8. Average Delay Time Comparison for Testing the Corresponding Model in Different Traffic Flow Scenarios.

3) *four-ring traffic flow*: According to the curve of Fig. 3 (c), the seeds are selected for the four-ring traffic flow. In this scenario, In order to simulate traffic conditions with low level of traffic congestion, we set the number of new vehicles added to the road network at each time step to 3. The other parameters of the simulator are set in the same way as other scenarios.

*Result Analysis.* The training curve in this scenario is shown in Fig. 6. The trained model is used to test in this scenario, and the test results are shown in Table IV. In this scenario, the training performance of IDQL is significantly better than that of IQL without double estimators. The learning process of Co-DQL, MA2C and DDPG is relatively stable and the standard deviation in the evaluation process is smaller than that of IQL and IDQL, this may be due to that these three methods share information in different ways among agents. But ultimately, Co-DQL achieves the shortest average delay time by means of mean field approximation for opponent modeling and local information sharing.

### C. Discussions

In order to more clearly assess the performance of various models under different traffic flow types and different level of traffic congestion, we make a direct comparison in Fig. 7 and Fig. 8. These figures show the results of our evaluation

in three scenarios, respectively, on mean episode reward and average delay time.

As seen from Fig. 7 (blue bar), all methods have a smaller mean episode reward in the global random traffic flow scene than in the other scenarios, which is due to the highest level of traffic congestion and the largest traffic volume in this scenario. According to Fig. 8 (green bar), although the mean episode reward level of each evaluation model in the four-ring traffic flow scenario is moderate, the average delay time of vehicles in this scenario is the longest, this may be due to the low level of traffic congestion and fewer vehicles, so although the total delay time may be not long, it may lead to higher average delay of vehicles.

Although the traffic volume of double-ring vehicle flow scene is larger than that of four-ring vehicle flow scene, the evaluation results in the former scene (orange bar) are even slightly better than the latter (green bar), regardless of the mean episode reward of agent or the average waiting time of vehicle. The analysis shows that the double-ring traffic flow scenario just needs the cooperation between two groups of agents, namely, the cooperation of signal agents in the inner and outer loop, while the four-ring traffic flow scenario needs the collaboration among four groups, so the cooperation task of signal agents in the latter may be more complex. Considering the three traffic scenarios, the effect of overestimation on the performance of the algorithm is different under various training tasks, but in general, the performance of the algorithms with double estimators is always better than that of the algorithms without double estimators. And in training and testing stage, Co-DQL can always make agents obtain more rewards and shorter average delay time than the state-of-the-art decentralized MARL algorithms.

## VI. CONCLUSION

When to design a multi-agent reinforcement learning algorithm, a critical challenge is how to make the agents efficiently cooperate, and one of the breach of realize is properly estimating the Q values and sharing local information among agents. Along this line of thought, this paper developed Co-DQL, which takes advantage of some important ideas studied in the literature. In more detail, Co-DQL employs an independent double Q-learning method based on double estimators and the UCB exploration, which can eliminate the over-estimation of traditional independent Q-learning while ensuring exploration. It adopts mean field approximation to model the interaction among agents in order to learn a better cooperative strategy. In addition, we presented a reward allocation mechanism and a local state sharing method. Based on the characteristics of TSC, we gave the details of the algorithmic elements. To validate the performance of the proposed algorithm, we tested Co-DQL on the multi-traffic signal simulator. Compared with several algorithms ( i.e., independent Q-learning, independent double Q-learning, DDPG and Multi-agent A2C), Co-DQL can provide promising results.

In the future, we hope to further test Co-DQL on the real signal networks. In addition, we will consider other approaches on large-scale multi-agent reinforcement learning such as hierarchical architecture [36] [37].

## ACKNOWLEDGMENT

This work was supported by the National Natural Science Foundation of China (No.61573277).

## REFERENCES

- [1] K.-L. A. Yau, J. Qadir, H. L. Khoo, M. H. Ling, and P. Komisarczuk, “A survey on reinforcement learning models and algorithms for traffic signal control,” *ACM Computing Surveys (CSUR)*, vol. 50, no. 3, p. 34, 2017.
- [2] Q. Wu and J. Guo, “Optimal bidding strategies in electricity markets using reinforcement learning,” *Electric Power Components and Systems*, vol. 32, no. 2, pp. 175–192, 2004.
- [3] B. Yin, M. Dridi, and A. El Moudni, “Traffic network micro-simulation model and control algorithm based on approximate dynamic programming,” *IET Intelligent Transport Systems*, vol. 10, no. 3, pp. 186–196, 2016.
- [4] P. Koonce and L. Rodegerdts, “Traffic signal timing manual.” United States. Federal Highway Administration, Tech. Rep., 2008.
- [5] H. Ceylan and M. G. Bell, “Traffic signal timing optimisation based on genetic algorithm approach, including drivers routing,” *Transportation Research Part B: Methodological*, vol. 38, no. 4, pp. 329–342, 2004.
- [6] J. García-Nieto, E. Alba, and A. C. Olivera, “Swarm intelligence for traffic light scheduling: Application to real urban areas,” *Engineering Applications of Artificial Intelligence*, vol. 25, no. 2, pp. 274–283, 2012.
- [7] J. Qiao, N. Yang, and J. Gao, “Two-stage fuzzy logic controller for signalized intersection,” *IEEE Transactions on Systems, Man, and Cybernetics-Part A: Systems and Humans*, vol. 41, no. 1, pp. 178–184, 2010.
- [8] D. Srinivasan, M. C. Choy, and R. L. Cheu, “Neural networks for real-time traffic signal control,” *IEEE Transactions on intelligent transportation systems*, vol. 7, no. 3, pp. 261–272, 2006.
- [9] R. S. Sutton and A. G. Barto, *Reinforcement learning: An introduction*. MIT press, 2018.
- [10] M. Wiering, J. v. Veenen, J. Vreeken, and A. Koopman, “Intelligent traffic light control,” 2004.
- [11] L. Prashanth and S. Bhatnagar, “Reinforcement learning with function approximation for traffic signal control,” *IEEE Transactions on Intelligent Transportation Systems*, vol. 12, no. 2, pp. 412–421, 2010.
- [12] Y. LeCun, Y. Bengio, and G. Hinton, “Deep learning,” *nature*, vol. 521, no. 7553, p. 436, 2015.
- [13] V. Mnih, K. Kavukcuoglu, D. Silver, A. A. Rusu, J. Veness, M. G. Bellemare, A. Graves, M. Riedmiller, A. K. Fidjeland, G. Ostrovski *et al.*, “Human-level control through deep reinforcement learning,” *Nature*, vol. 518, no. 7540, p. 529, 2015.
- [14] T. P. Lillicrap, J. J. Hunt, A. Pritzel, N. Heess, T. Erez, Y. Tassa, D. Silver, and D. Wierstra, “Continuous control with deep reinforcement learning,” *arXiv preprint arXiv:1509.02971*, 2015.
- [15] H. Wei, G. Zheng, H. Yao, and Z. Li, “Intellilight: A reinforcement learning approach for intelligent traffic light control,” in *Proceedings of the 24th ACM SIGKDD International Conference on Knowledge Discovery & Data Mining*. ACM, 2018, pp. 2496–2505.
- [16] N. Casas, “Deep deterministic policy gradient for urban traffic light control,” *arXiv preprint arXiv:1703.09035*, 2017.
- [17] C. Claus and C. Boutilier, “The dynamics of reinforcement learning in cooperative multiagent systems,” *AAAI/IAAI*, vol. 1998, no. 746-752, p. 2, 1998.
- [18] S. Shamshirband, “A distributed approach for coordination between traffic lights based on game theory,” *Int. Arab J. Inf. Technol.*, vol. 9, no. 2, pp. 148–153, 2012.
- [19] I. Arel, C. Liu, T. Urbanik, and A. Kohls, “Reinforcement learning-based multi-agent systems for network traffic signal control,” *IET Intelligent Transport Systems*, vol. 4, no. 2, pp. 128–135, 2010.
- [20] M. Abdoos, N. Mozayani, and A. L. Bazzan, “Traffic light control in non-stationary environments based on multi agent q-learning,” in *2011 14th International IEEE conference on intelligent transportation systems (ITSC)*. IEEE, 2011, pp. 1580–1585.
- [21] M. Tan, “Multi-agent reinforcement learning: Independent vs. cooperative agents,” in *Proceedings of the tenth international conference on machine learning*, 1993, pp. 330–337.
- [22] L. Kuyer, S. Whiteson, B. Bakker, and N. Vlassis, “Multiagent reinforcement learning for urban traffic control using coordination graphs,” in *Joint European Conference on Machine Learning and Knowledge Discovery in Databases*. Springer, 2008, pp. 656–671.
- [23] T. Chu, J. Wang, L. Codecà, and Z. Li, “Multi-agent deep reinforcement learning for large-scale traffic signal control,” *IEEE Transactions on Intelligent Transportation Systems*, 2019.
- [24] H. V. Hasselt, “Double q-learning,” in *Advances in Neural Information Processing Systems*, 2010, pp. 2613–2621.
- [25] P. Auer, N. Cesa-Bianchi, and P. Fischer, “Finite-time analysis of the multiarmed bandit problem,” *Machine learning*, vol. 47, no. 2-3, pp. 235–256, 2002.
- [26] H. E. Stanley, *Phase transitions and critical phenomena*. Clarendon Press, Oxford, 1971.
- [27] Y. Yang, R. Luo, M. Li, M. Zhou, W. Zhang, and J. Wang, “Mean field multi-agent reinforcement learning,” *arXiv preprint arXiv:1802.05438*, 2018.
- [28] H. Van Hasselt, A. Guez, and D. Silver, “Deep reinforcement learning with double q-learning,” in *Thirtieth AAAI conference on artificial intelligence*, 2016.
- [29] J. E. Smith and R. L. Winkler, “The optimizers curse: Skepticism and postdecision surprise in decision analysis,” *Management Science*, vol. 52, no. 3, pp. 311–322, 2006.
- [30] L. S. Shapley, “Stochastic games,” *Proceedings of the national academy of sciences*, vol. 39, no. 10, pp. 1095–1100, 1953.
- [31] M. L. Littman, “Markov games as a framework for multi-agent reinforcement learning,” in *Machine learning proceedings 1994*. Elsevier, 1994, pp. 157–163.
- [32] M. Li, Z. Qin, Y. Jiao, Y. Yang, J. Wang, C. Wang, G. Wu, and J. Ye, “Efficient ridesharing order dispatching with mean field multi-agent reinforcement learning,” in *The World Wide Web Conference*. ACM, 2019, pp. 983–994.
- [33] T. Jaakkola, M. I. Jordan, and S. P. Singh, “Convergence of stochastic iterative dynamic programming algorithms,” in *Advances in neural information processing systems*, 1994, pp. 703–710.
- [34] C. Szepesvári and M. L. Littman, “A unified analysis of value-function-based reinforcement-learning algorithms,” *Neural computation*, vol. 11, no. 8, pp. 2017–2060, 1999.
- [35] G. Brockman, V. Cheung, L. Pettersson, J. Schneider, J. Schulman, J. Tang, and W. Zaremba, “Openai gym,” *arXiv preprint arXiv:1606.01540*, 2016.
- [36] T. Tan, F. Bao, Y. Deng, A. Jin, Q. Dai, and J. Wang, “Cooperative deep reinforcement learning for large-scale traffic grid signal control,” *IEEE transactions on cybernetics*, 2019.
- [37] A. S. Vezhnevets, S. Osindero, T. Schaul, N. Heess, M. Jaderberg, D. Silver, and K. Kavukcuoglu, “Feudal networks for hierarchical reinforcement learning,” in *Proceedings of the 34th International Conference on Machine Learning-Volume 70*. JMLR. org, 2017, pp. 3540–3549.